# A NEW APPROACH FOR OPTIMISING SATELLITE SHIELDING AND CONFIGURATION USING GENETIC ALGORITHMS

P.H. Stokes, R. Crowther, V. Marsh, and R.J. Walker

Space Debris Group, Space Department, Defence Research Agency,
Farnborough, Hampshire, GU14 0LX, UK

G.G. Swinerd

Department of Aeronautics and Astronautics, University of Southampton,
Southampton, Hampshire, SO17 1BJ, UK

## ABSTRACT

Consideration of cost-effective shielding is now an essential element in the design of a satellite system. To minimise the vulnerability to debris and meteoroid impact a designer may choose to add physical shielding and/or reposition critical components or subsystems. Traditionally, these decisions have necessitated a degree of engineering judgement. The uncertainties associated with such an approach may lead to a non-optimal shielding solution being implemented in the design. To overcome this a new model is being developed which will identify the cost-optimum protection solution using an automated search method based on genetic algorithm theory. A prototype of the model has demonstrated the feasibility of the technique. Preliminary results suggest an interdependency between the choice and location of external physical shielding and the arrangement of internal components. This emphasises the importance of considering appropriate protection measures at the earliest opportunity in the satellite design process.

## 1. INTRODUCTION

An accurate knowledge of the debris and meteoroid environment and its effect is crucial if the survivability of a satellite system is to be maximised and the associated costs of protection minimised. A manufacturer must know if a proposed satellite configuration is particularly vulnerable to debris and meteoroid impacts, and if necessary take corrective action. Possible solutions for improving a vulnerable design are: the addition of physical shielding, repositioning of critical components, or some combination of the two. Traditionally, a degree of engineering judgement, coupled with the results of impact simulations, is used to decide the best arrangement of components and shielding. Such an approach may lead to a reasonably good design, but it does not guarantee that the most cost-effective protection strategy has been implemented, and it does not reflect other design constraints such as secondary radiation effects. In this paper we introduce a new model for identifying the cost-optimum solution using an automated search technique based on genetic algorithm theory. A prototype of the model is currently being developed in accordance with ESA Software Engineering Standards (Ref. 1) to demonstrate the concept. It simultaneously identifies the optimum physical shielding external to a satellite body in conjunction with the optimum arrangement of components inside the body. Such a concurrent engineering approach ensures that critical components are afforded cost-optimum protection from those impactors which might penetrate the satellite body.

## 2. DESCRIPTION OF MODEL

The model requires two inputs - an accurate geometrical representation of the satellite body and its internal components, and a distribution of the particles which impact the external surfaces of the geometry during its mission life. The particle distribution can be derived from impact flux data, which is available from impact simulators such as ESABASE/DEBRIS or BUMPER. For the prototype demonstrator model we have simplified matters by using a simple 2D geometry together with a randomly generated impact distribution. The simulation begins by creating a random population of competing designs. Each solution has a unique arrangement of internal components together with a unique combination of shielding protecting the outside of the satellite body. Four types of shield can be selected: single wall (i.e. the body structure), Whipple, mesh double bumper, and multi-shock shield.

### 2.1 Survivability metric

Each of the competing solutions is evaluated to determine its survivability, or 'fitness' to survive the environment. We do this by defining a survivability metric, the derivation of which is a three step process.

### 2.1.1 Survivability metric derivation - step 1

Using equations in the literature (Refs. 2 - 6), we calculate which of the particles from the impact distribution penetrate the satellite body (and shielding). Each of the penetrators generates a cloud of secondary debris inside the body. An expanding debris cloud defines, to a first approximation, the volume of internal space most at risk, i.e. a 'vulnerability cone'. Any components lying within the vulnerability cone will be susceptible to damage. To define a cone we calculate the trajectory and spray angle of the secondary debris cloud from equations such as those listed in Refs. 4, 7 - 9. The exact region of space lying within a cone can be identified by applying a mesh to the satellite body, and calculating which of the grid elements lie within the cone. Each of these grid elements can then be assigned a 'vulnerability metric' to distinguish it as a region of higher vulnerability (see Fig. 1).

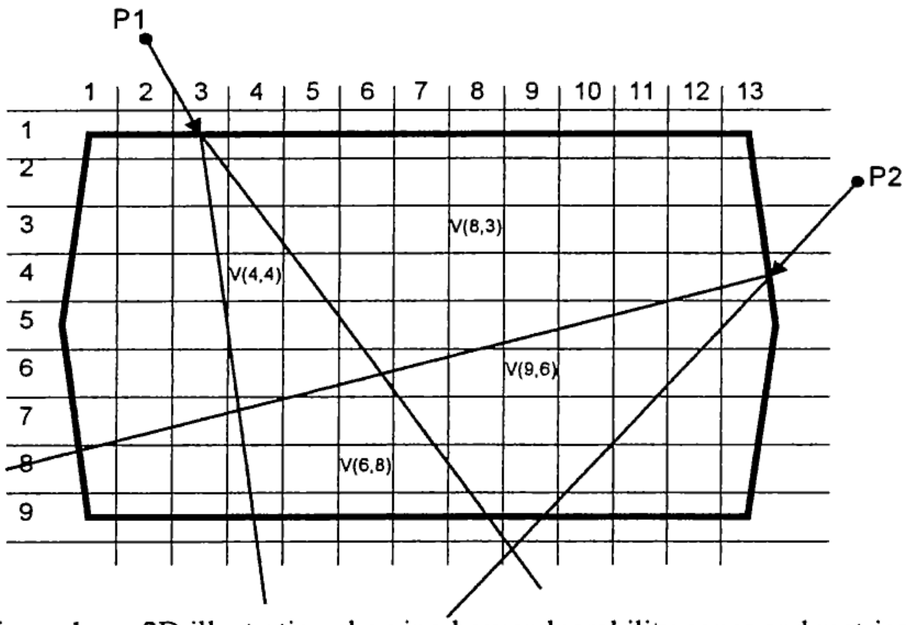


Figure 1. 2D illustration showing how vulnerability cones and metrics define regions of high impact risk

The region of space occupied by grid element (6,8) is vulnerable to impact from two debris clouds, thus increasing its vulnerability metric. However, the element is located well away from the impact points; so only a small percentage of the cloud energies will pass through the element. Therefore, the vulnerability of element (6,8) may in fact be less than element (4,4). Based on this logic we can define the vulnerability metric as follows:

$$V(m,n) = \sum_{i=1}^{I} E_i \left[ \frac{A(m,n)}{A_i} \right] \qquad (1)$$

where V(m,n) is the vulnerability metric for grid element (m,n), $E_i$ is the energy of penetrating impactor *i*, A(m,n) is the mean cross-sectional projected area of grid element (m,n), and $A_i$ is the surface area of the debris cloud generated by penetrating impactor *i*. Fig. 2 illustrates this calculation for grid element (6,8).

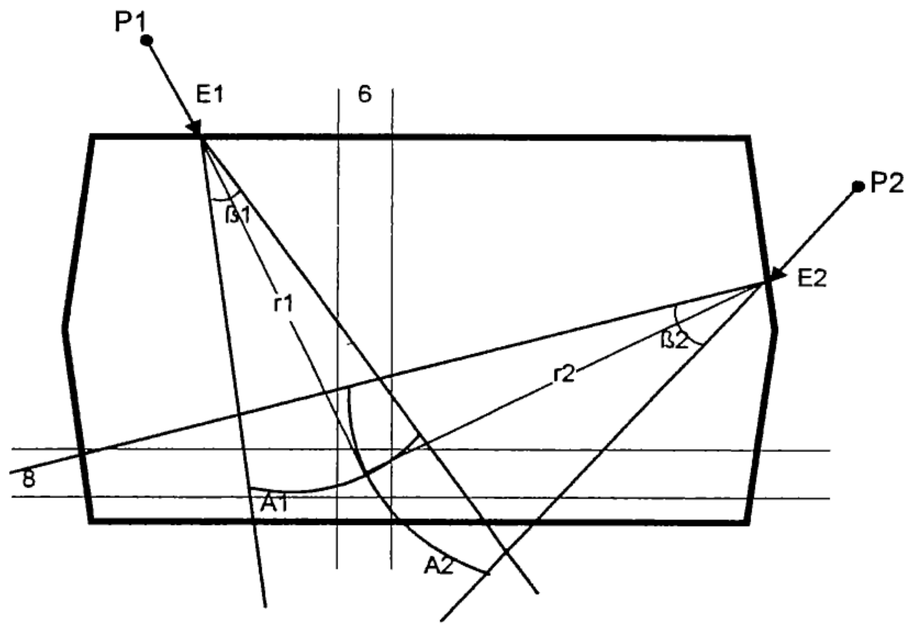


Figure 2. 2D illustration showing how a grid element vulnerability metric is calculated

The area $A_i$ refers to that part of the surface of a sphere (radius $r_i$) contained within a vulnerability cone of spread angle $\beta_i$. Therefore, we assume that all of the material within the debris cloud is spread evenly over this area.

Once all grid element metrics have been calculated in this manner, we will have a 2D vulnerability matrix, or map, which characterises the most vulnerable internal regions of the satellite body.

### 2.1.2 Survivability metric derivation - step 2

In the second step of the derivation we overlay each of the components onto the map, thereby enabling their vulnerabilities to be calculated (see Fig. 3).

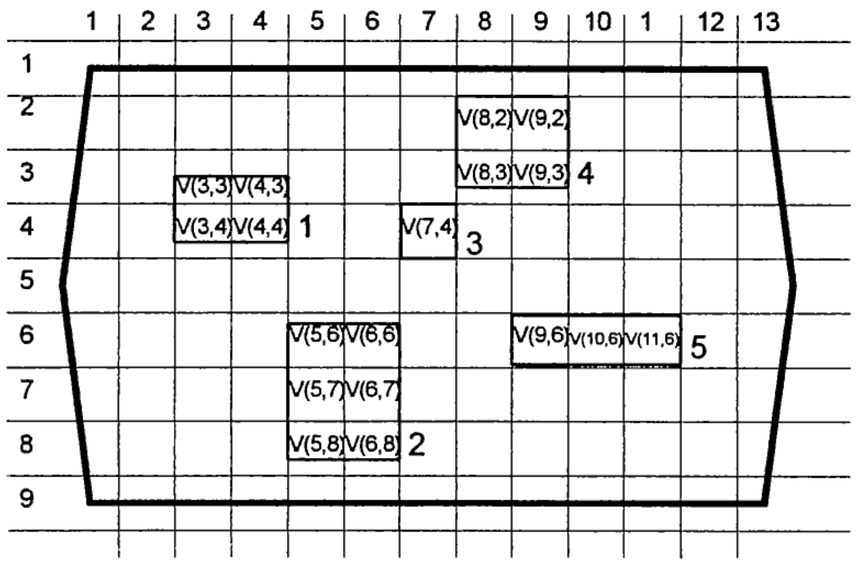


Figure 3. 2D illustration showing how component vulnerability metrics are calculated

For example, the vulnerability metric for component 1 is calculated by summing the metrics of the four grid elements it overlays, i.e.:

$$V_1 = V(3,3) + V(4,3) + V(3,4) + V(4,4) \qquad (2)$$

From the preceding definitions, one can see that this vulnerability metric is related to the total amount of impact energy that the component has to absorb assuming no other internal components are present. Of course, in practice there are probably many internal components which could absorb some of this energy. In fact, the more a component is surrounded by others, the less likely it is that it will have to absorb the energy from penetrative impactors. Therefore, we have to modify the component vulnerability metric to take this into account. To do this, we introduce a 'protection factor'. For each component, a ray is fired from its centre to the body structure, and then swept through 360° in 1° steps, rather like a radar sweep. Each time the ray encounters a component the protection factor is incremented. We can express this mathematically as follows:

$$P_j = \left[ \sum_{k=1}^{360} \sum_{l} R_l \right] \tag{3}$$

where $P_j$ is the protection factor for component $j$, $k$ is the angle swept out by the ray in degrees, and $R_l$ is the impact resistance of an intervening component $l$. If we assume that all internal components are electronic boxes with approximately equal resistance then we can normalise the value of R to 1 for each component.

Finally, we introduce a dimensionless factor called the component 'criticality'. Clearly, a component that is very susceptible to impact should be a cause for concern if it is critical to mission success. However, a non-critical item with the same susceptibility does not merit the same level of concern. Therefore, a criticality factor provides a means of distinguishing between these two cases. We define the component criticality factor as follows:

$$Q_j = \frac{X_j}{100} \tag{4}$$

where $Q_j$ is the criticality of component $j$, and $X_j$ is the percentage mission loss if component $j$ is lost. The evaluation of $X_j$ is based largely on engineering judgement, drawing on reliability analysis techniques such as Failure Modes Effects and Criticality Analysis (FMECA).

### 2.1.3 Survivability metric derivation - step 3

The combination of vulnerability metric, protection factor and criticality factor is sufficient to characterise the susceptibility of each internal component, and therefore the survivability of the overall spacecraft design. We define a metric to represent the spacecraft survivability as follows:

$$S = \sum_{j=1}^{J} \frac{P_j Q_j}{1 + V_j} \tag{5}$$

If required, the spacecraft survivability metric can be adjusted to take into account the cost of applying any direct shielding to the spacecraft design. The addition of physical shielding not only increases the cost of constructing the satellite, but also increases the mass of the satellite. This is turn implies an increase in the cost to launch the satellite. To address this we have devised the following metric for cost-effective survivability:

$$S = \left[ \sum_{j=1}^{J} \frac{P_j Q_j}{(1 + V_j)} \right] \Big/ \left[ C_B + C_{Sh} + \beta \left( M_B + M_{Sh} \right)^{\alpha} \right] \tag{6}$$

where $C_B$ is the manufacturing cost of the satellite body structure, $C_{Sh}$ is the total manufacturing cost of all external shielding, $M_B$ is the body mass, $M_{Sh}$ is the total mass of shielding, and $\alpha$ and $\beta$ are dimensionless factors relating launch cost to mass. We shall use this definition of survivability to quantify the effectiveness of a particular protection strategy, and thereby enable comparisons between competing design solutions.

## 2.2 Genetic algorithm process

With each design in the initial population evaluated in this manner, the model converts the designs into a population of 'chromosomes' ranked according to their 'fitness'. A chromosome consists of a string of 'genes' which have been concatenated. A gene represents a variable in the design, in this case a component location or a shield type. For example, a design with 10 components would be converted into a chromosome of 10 genes, with each gene being a component location point. Each gene is converted into a binary number; so the chromosome could look as follows:

| Gene A | Gene B | Gene C | Gene D | |
|---|---|---|---|---|
| 10010 | 01011 | 11100 | 00101 | etc.... |
| Comp. 1 | Comp. 2 | Comp. 3 | Comp. 4 | |

That is, a long string of binary digits. This process is repeated for each of the design solutions in the randomly generated population. Three standard genetic

algorithm operations are then performed on the population of chromosomes, namely selection, crossover, and mutation, to create a new population of 'child' chromosomes (Ref. 10).

Selection occurs when two chromosomes are chosen from the population using a selection operator which is designed to pick out the 'fittest' chromosomes from the population more frequently. During crossover the two selected chromosomes are 'mated', i.e. information is swapped between the chromosomes to create two new 'child' chromosomes. This information is in the form of a segment of binary digits from the chromosome strings, as illustrated below:

Parent chromosome 1

| 10110 | 01011 | 10101 | 00100 | etc.... |
|---|---|---|---|---|

|←——— Segment →|

Parent chromosome 2

| 01010 | 10101 | 11011 | 10011 | etc.... |
|---|---|---|---|---|

|←——— Segment →|

Child chromosome 1

| 10010 | 10101 | 11011 | 00100 | etc.... |
|---|---|---|---|---|

Child chromosome 2

| 01110 | 01011 | 10101 | 10011 | etc.... |
|---|---|---|---|---|

Finally, the child chromosomes are mutated slightly to diversify the population. This simply involves randomly changing a binary digit in each chromosome from zero to one, or vice versa.

The above sequence of operations is repeated until a completely new generation of child chromosomes has been created, equal in size to the original parent population. The two best parent chromosomes are added to this new population of children to ensure that the optimum is retained at all times.

Each child chromosome is then converted back into a design. The survivability metrics of these child designs are evaluated in exactly the same fashion as the initial population of 'parents'. After repeating this process for N generations, it can be shown that the final population contains a design solution which is close to the global optimum.

## 3. RESULTS

Preliminary results from running the prototype model show that it can search out a near-global optimum design solution within 100 generations, where each generation comprises 100 competing designs. In the example simulation in Figs. 4 and 5 the model is optimising a satellite comprising 9 internal components, all of which are identical with the exception that one component has a criticality of 90% compared to 10% for the others. All four choices of external shielding described earlier are available to protect the body, and we have assumed that the cost per unit mass of each shield option is the same.

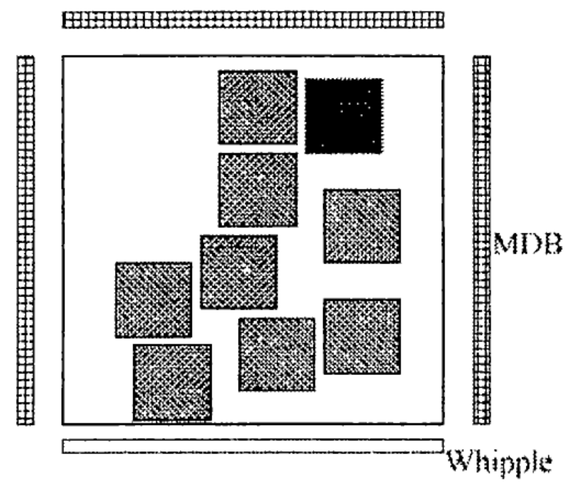


Figure 4 Best design in initial population

Fig. 4 shows the best design in the initial randomly generated population, with a survivability metric of 0.0028. The external shielding comprises a mixture of mesh double bumper (MDB) and Whipple bumper. Inside the body the components are well spread out, and the critical component is quite exposed and vulnerable to impact. After 100 generations the best design has a survivability metric of 0.0364, a factor of 13 improvement. The preferred method of external shielding on each face is mesh double bumper, and the internal components are clustered together to provide an improved degree of protection to the critical component (see Fig. 5).

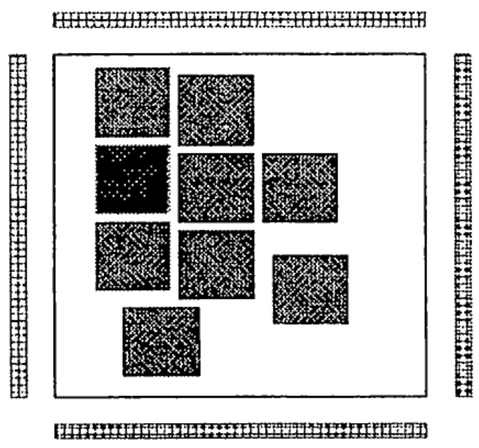

Figure 5 Best design in final population

We can confirm that this internal arrangement is credible by examining the vulnerability map inside the satellite body (see Fig. 6). The large lighter shaded area represents the region of lowest vulnerability. As expected, the components have a tendency to occupy this region.

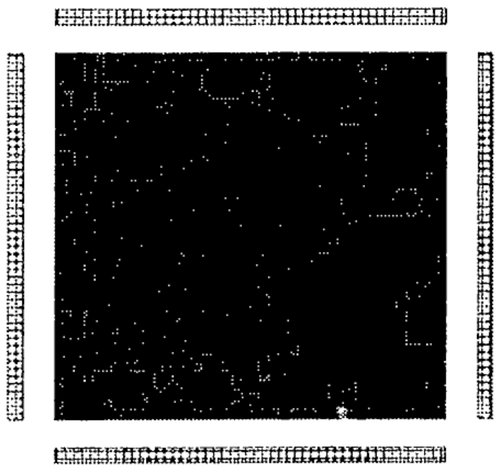

Figure 6 Vulnerability map inside satellite body

The ease with which the model was able to converge on the near-optimum solution is illustrated by examining the growth in survivability metric throughout the generations. Fig. 7 shows how the metric for the best design in each generation increases rapidly at first, followed by smaller increases later on. This is a good indication that the model is efficient at focusing in on the near-optimum solution.

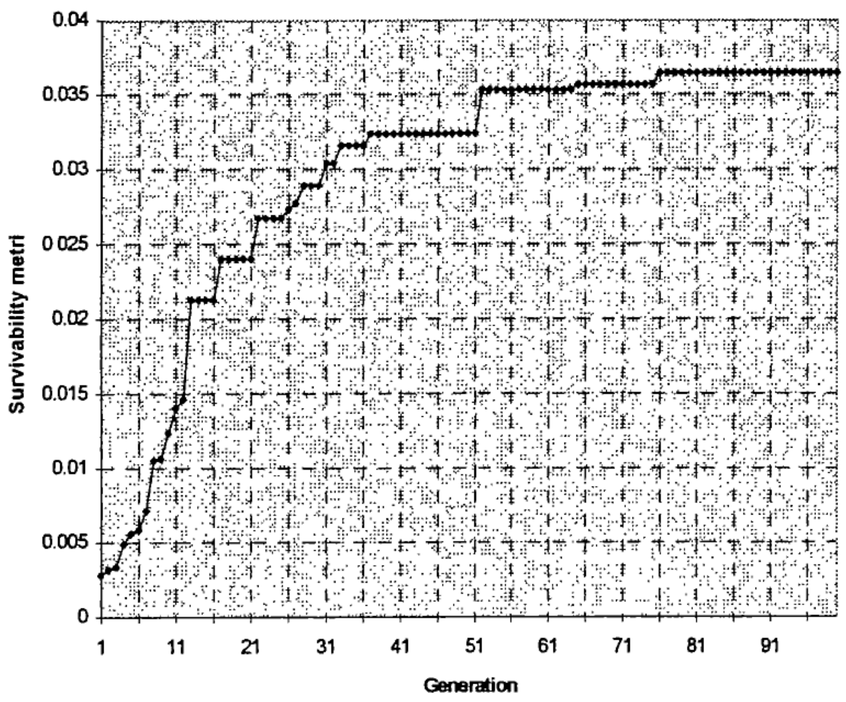


Figure 7 Survivability metric for best design in each generation

In practice the design solution in Fig. 5 would probably not be feasible because of poor mass balance and thermal balance. It is possible to consider constraints such as these by making the appropriate modification to the survivability metric. For example, to include a mass balance constraint, the metric in Eq. 6 can be modified as follows

$$S = \left[\frac{r_{\max} - r_a}{r_{\max}}\right] \text{x} \left[\sum_{j=1}^{J} \frac{P_j Q_j}{(1+V_j)}\right] \Big/ \left[C_B + C_{Sh} + \beta\left(M_B + M_{Sh}\right)^{\alpha}\right] \quad (7)$$

where $r_a$ is the distance of the actual centre of mass of the body from the desired position, and $r_{max}$ is the maximum possible distance that the centre of mass can deviate from the desired position. Repeating the earlier example simulation we derive a new optimum design solution (see Fig. 8).

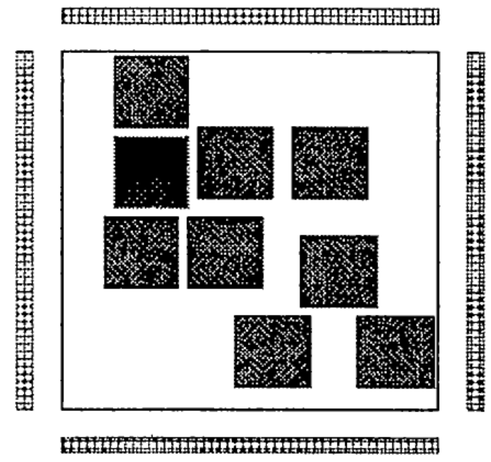

Figure 8 Best design in final population (subject to mass balance constraint)

The effect of including the mass balance constraint is clearly shown. The critical component is still located in the lowest vulnerability region, and is well protected by neighbouring non-critical components. However, two of the non-critical components now occupy more vulnerable regions, thereby improving the mass balance of the design. The resulting optimum solution is therefore an illustration of the compromise between the need for protection and the need to satisfy constraints on the design.

## 4. CONCLUSIONS

Initial results from the prototype model have demonstrated that the genetic algorithm technique, coupled with the definition of satellite survivability metric, is an efficient method for achieving a cost optimum protection solution.

Results have confirmed that there is a strong inter-dependency between the choice and location of external physical shielding and the location of critical components inside the satellite body. The derivation of an optimum protection solution can only be achieved by simultaneously considering both of these factors. This emphasises the importance of considering appropriate protection measures during the early phases of a satellite design, rather than as an add-on extra in the later stages.

The ease with which the prototype was successfully extended to include a design constraint, i.e. satellite mass balance, suggests that the modelling approach could be used to address more complex optimisations. For example, to properly optimise the external shielding

and location of internal components for maximum cost-effective protection, one needs to consider secondary radiation effects as well as debris and meteoroid impacts. Furthermore, constraining factors such as good thermal balance and vibration integrity must also be included. Traditional design methodologies usually address each of these problems individually and sequentially until a satisfactory (not necessarily cost-optimum) design solution is attained. Our approach benefits by being able to address these problems simultaneously, thus ensuring that we focus on the optimum design.

## 5. FURTHER WORK

Continued development and further runs of the prototype are anticipated. In particular, a sensitivity analysis of the survivability metric will help us to understand the relative importance of various terms, and may identify areas for improvement. A more precise formulation of the expanding secondary debris clouds, in terms of mass, energy, momentum, shape and material state (Refs. 11, 12), is also planned.

Once prototyping is complete, work will begin on the development of a full debris, meteoroid and radiation protection model. This will incorporate 3D geometries, and relevant constraining factors. Enhancements of the genetic algorithm are also envisaged to increase its efficiency at focusing on the global optimum solution.

Finally, it is worth mentioning two external areas of research upon which our model is dependent, and for which data is lacking. First, there are a limited number of empirical secondary debris equations. This restricts the accuracy of the internal vulnerability map in our model. Indeed, it has proved very difficult to identify a comprehensive set of equations which fully characterise the impact response of a range of shield options, particularly in terms of secondary debris clouds released following penetration. Therefore it is important that future impact test programmes collect data on secondary ejecta as a matter of routine. Information which just characterises the shield damage is not sufficient to determine whether the shield is cost-effective. Second, our model also requires information on the relative impact resistance of internal components. Such data is not widely available, but could be acquired from a relatively inexpensive test programme.

## 6. REFERENCES

1. Mazzo, C., Fairclough, J., Melton, B., De Pablo, D., Scheffer, A., and Stevens, R., *Software Engineering Standards*, European Space Agency PSS-05-0, 1994.

2. Berthoud, L., and Mandeville, J. C., Empirical Impact Equations and Marginal Perforation, *Proc. First European Conference on Space Debris*, Darmstadt, Germany, ESA SD-01, 5-7 April 1993.

3. Christiansen, E. L., Performance Equations for Advanced Orbital Debris Shields, *AIAA Space Programs and Technologies Conference*, Huntsville, Alabama, AIAA 92-1462, 1992.

4. Elfer, N. C., Structural Damage Prediction and Analysis for Hypervelocity Impacts - Handbook, *NASA Contractor Report 4706*, Feb. 1996.

5. Destefanis, R., and Callea, M., Meteoroid and Debris Impacts on Orbiting Structures: A Methodology, *Proc. First European Conference on Space Debris*, Darmstadt, Germany, ESA SD-01, 5-7 April 1993.

6. Reimerdes, H-G., Stecher, K-H., and Lambert, M., Ballistic Limit Equations for the Columbus Double Bumper Shield Concept, *Proc. First European Conference on Space Debris*, Darmstadt, Germany, ESA SD-01, 5-7 April 1993.

7. Lambert, M., Shielding Against Orbital Debris - A Challenging Problem, *Proc. ESA Symposium on Space Applications of Advanced Structural Materials*, ESTEC, Noordwijk, NL, ESA-SP-303, June 1990.

8. Lawrence, R. J., A Simple Approach for the Design and Optimisation of Stand-off Hypervelocity Particle Shields, *AIAA Space Programs and Technologies Conference*, Huntsville, Alabama, AIAA Paper 92-1465, March 1992.

9. Schonberg, W. P., and Bean, A. J., Hypervelocity Impact Physics, *NASA Contractor Report 4343*, 1991.

10. Davis, L., *Handbook of Genetic Algorithms*, International Thomson Publishing Inc., 1991.

11. Herrmann, W., and Wilbeck, J. S., Review of Hypervelocity Penetration Theories, *Int. J. Impact Engng*, Vol. 5, 1987.

12. Schonberg, W. P., Characterising Material States in Orbital Debris Impacts, *Proc. SPIE Conference on Space Environmental, Legal, and Safety Issues*, Orlando, Florida, 17-18 April 1995.